



An Alternative Variational Calculation of the Trapping Rate in Thermal Barriers

X.Z. Li and G.A. Emmert

July 1983

UWFDM-524

***FUSION TECHNOLOGY INSTITUTE
UNIVERSITY OF WISCONSIN
MADISON WISCONSIN***

DISCLAIMER

This report was prepared as an account of work sponsored by an agency of the United States Government. Neither the United States Government, nor any agency thereof, nor any of their employees, makes any warranty, express or implied, or assumes any legal liability or responsibility for the accuracy, completeness, or usefulness of any information, apparatus, product, or process disclosed, or represents that its use would not infringe privately owned rights. Reference herein to any specific commercial product, process, or service by trade name, trademark, manufacturer, or otherwise, does not necessarily constitute or imply its endorsement, recommendation, or favoring by the United States Government or any agency thereof. The views and opinions of authors expressed herein do not necessarily state or reflect those of the United States Government or any agency thereof.

An Alternative Variational Calculation of the Trapping Rate in Thermal Barriers

X.Z. Li and G.A. Emmert

Fusion Technology Institute
University of Wisconsin
1500 Engineering Drive
Madison, WI 53706

<http://fti.neep.wisc.edu>

July 1983

UWFDM-524

AN ALTERNATIVE VARIATIONAL CALCULATION
OF THE TRAPPING RATE IN THERMAL BARRIERS

X.Z. Li

G.A. Emmert

Fusion Engineering Program
Department of Nuclear Engineering
University of Wisconsin
Madison, Wisconsin 53706

July 1983

UWFD-524

Abstract

A variational calculation of the trapping rate and trapped ion density in thermal barriers is presented. The effects of diffusion in energy as well as pitch angle scattering are retained. The variational formulation uses the actual trapped-passing boundary in velocity space. The boundary condition is that the trapped ion distribution function match the passing ion distribution function, which is taken to be a Maxwellian, on the boundary. The results compare well with two-dimensional Fokker-Planck code calculations by Futch and LoDestro. The CPU time for a variational calculation is less than 0.1 sec using the CRAY-I computer, while a typical Fokker-Planck code calculation takes 10-20 minutes.

1. Introduction

The thermal barrier⁽¹⁾ is a recently introduced concept in tandem mirrors. It is a region of depressed potential between the central cell and the plug; the thermal barrier reduces the rate of energy transfer⁽²⁾ between the plug and central cell electrons and thereby allows one to heat the plug electrons without excessive heating of the central cell electrons.

A fundamental problem is the trapping of ions in thermal barriers. Trapped ions increase the electron density in the thermal barrier (through quasi-neutrality) and thereby reduce the magnitude of the potential depression; this reduces the effectiveness of the thermal barrier. In order to remove the trapped ions, a "pumping" mechanism is required. One such method for pumping the thermal barrier is to inject a neutral beam at the appropriate energy and angle.⁽³⁾ Charge exchange between the trapped ions and the injected neutral atoms removes trapped ions and replaces them with "passing" (i.e., they can pass back into the central cell) ions. Alternative techniques using drift orbits,^(4,5) or induced radial losses of the trapped ions by time-varying fields⁽⁶⁾ have also been proposed. In a previous paper⁽⁷⁾ we attempted to set up a model for the drift pumping case. In this paper we treat the neutral beam pumping case.

Numerical calculations of the trapping rate in thermal barriers have been done by Futch and LoDestro⁽⁸⁾ using Fokker-Planck codes. Carrera and Callen⁽⁹⁾ have given an analytical calculation of the trapping rate using a pitch-angle scattering collision operator; diffusion in energy was neglected. In an earlier paper⁽¹⁰⁾ we presented a variational calculation of the trapping rate. In this paper we present an alternative variational calculation which has a better theoretical foundation, is faster, and just as accurate as the

earlier variational calculation. The variational calculations allow a better treatment of the boundary condition and include the effect of energy diffusion. The results are generally in good agreement with the numerical Fokker-Planck code results in both the high and low barrier mirror ratio cases.

The variational method has been used to calculate the end-loss from a central cell where the ions are confined by the combination of an electrostatic potential and a magnetic mirror. Figure 1 shows contour lines for the ion distribution function in a thermal barrier and in the central cell of a tandem mirror. In the central cell case, the "loss-cone" is essentially empty, so that the boundary condition normally taken is that the ion distribution function, f , vanish on the loss-cone boundary. Since the confining potential is normally large compared with the ion temperature, the bulk of the ions have a Maxwellian distribution and the deformation caused by the loss-cone appears primarily in the high energy "tail" of f . The problem of the diffusion current into the loss-cone was solved first by Pastukhov.⁽¹¹⁾ Later, Chernin and Rosenbluth⁽¹²⁾ used a variational method to obtain the diffusion rate. Catto and Bernstein⁽¹³⁾ improved the variational calculation with a better treatment of the boundary condition and extended it to the bounce-averaged Fokker-Planck equation. All of these calculations used the fact that the bulk of the ion distribution is nearly Maxwellian; the field particle distribution in the Fokker-Planck equation can be assumed to be Maxwellian. This linearizes the Fokker-Planck equation and allows one to formulate a variational functional.

In the thermal barrier, the situation is rather different. The passing ions are assumed to have a Maxwellian distribution since they have come from

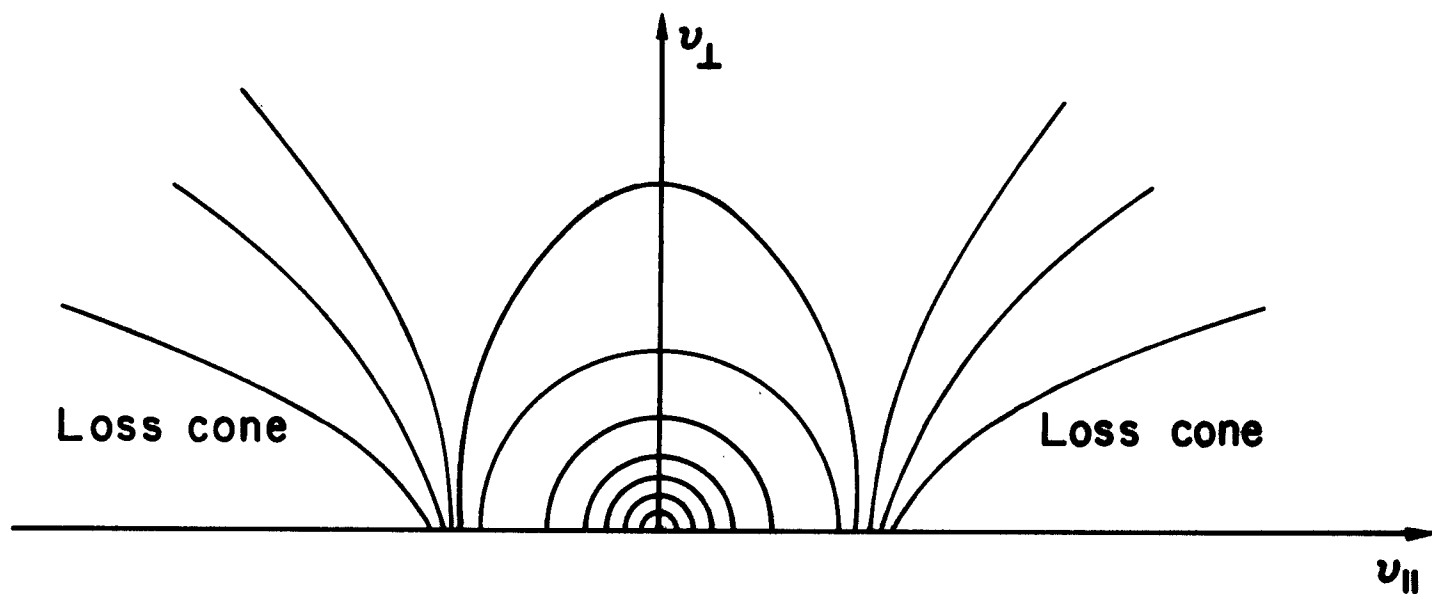
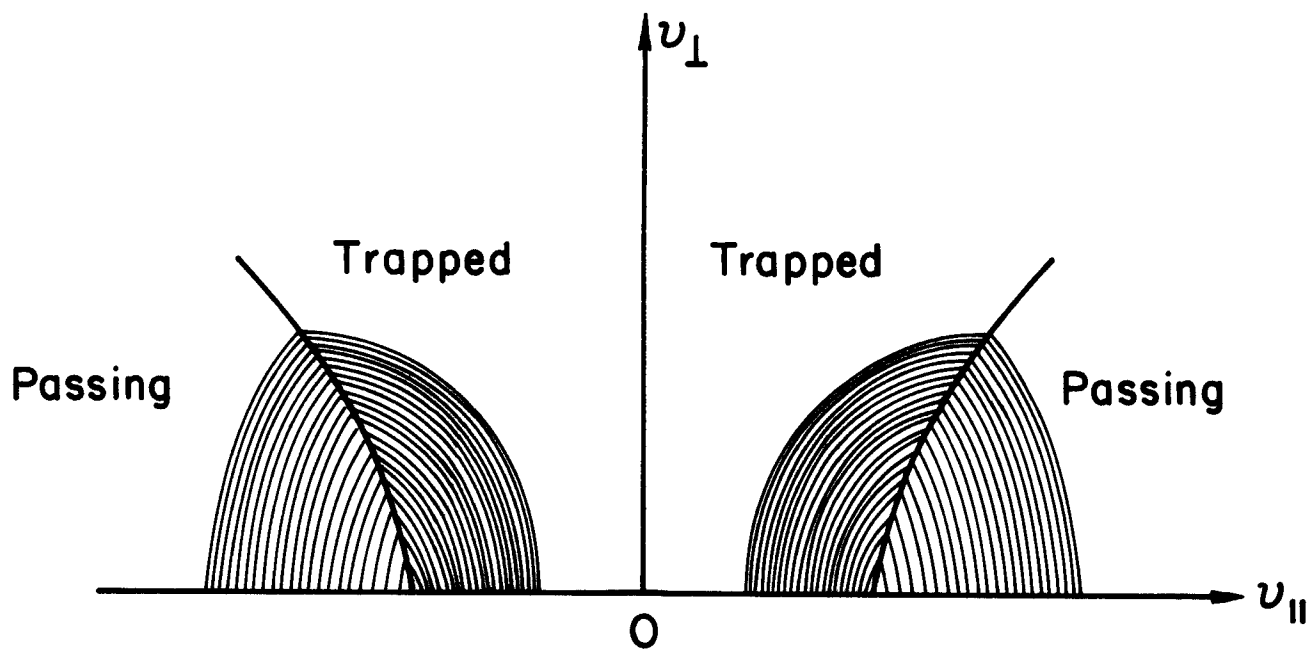


Fig. 1 Velocity space for the thermal barrier (upper diagram) and the central cell (lower diagram).

the central cell. The trapped ions, however, are concentrated near the trapped-passing boundary. The density of the trapped ions is about the same as for the passing ions. Consequently, linearization of the Fokker-Planck equation is not so straightforward. Furthermore, one now requires that the trapped particle distribution function match the Maxwellian distribution of the passing ions on the trapped-passing boundary. This boundary condition also presents some complications. In our earlier report we formulated a variational treatment of this problem. In this report, we obtain the variational functional in a different way and use a different trial function to estimate the stationary value of the functional and, thereby, the trapping current. This method requires about 0.1 sec on the CRAY computer to calculate the trapping current; our earlier method required about 1 sec. Both of these compare well with the 10-20 minutes required for the large Fokker-Planck code calculations.

2. Formulation of the Problem

We model the magnetic field and the potential in the thermal barrier as a square well, as shown in Fig. 2. The boundary in velocity space between ions which are trapped in the thermal barrier and ions which can pass back into the central cell (i.e., "passing" ions) is shown in Fig. 1. This boundary is given by

$$v_{\parallel}^2 + v_{\perp}^2(1 - R_b) - v_b^2 = 0 \quad (2.1)$$

where

$$R_b = B_{mb}/B_b, \quad v_b^2 = \frac{2\phi_b}{m} \quad (2.2)$$

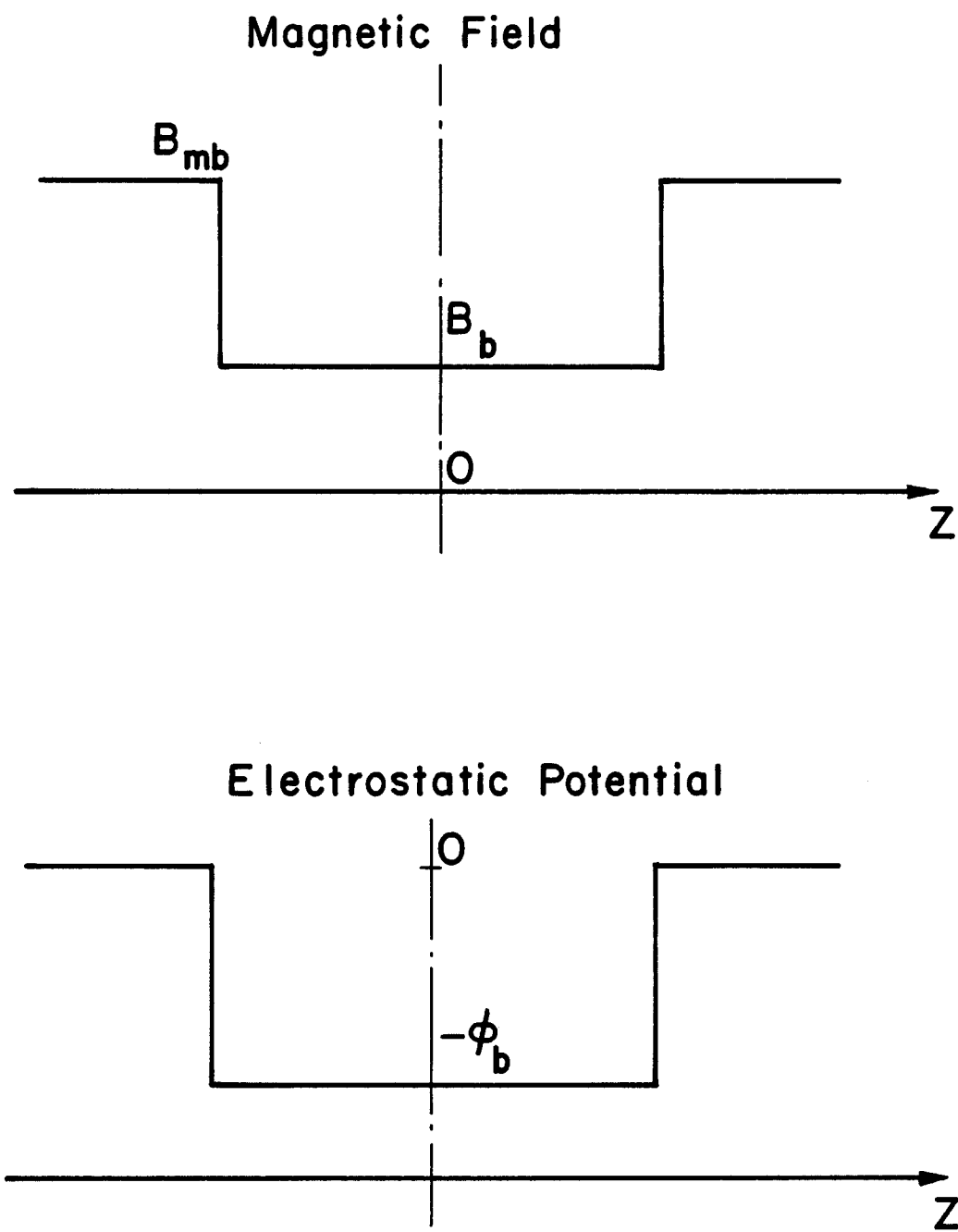


Fig.2 Square well model for the thermal barrier.

and v_{\parallel} , v_{\perp} are measured at the bottom of the barrier. Here, potential and temperature are measured in units of energy, and m is the ion mass.

The kinetic equation for the trapped ion distribution function, f , is

$$-\vec{\nabla} \cdot \vec{I} - \nu f = 0 \quad (2.3)$$

where \vec{I} is the diffusion current in velocity space and charge exchange pumping is modeled as an "absorption" term with a constant coefficient ν , which has units of sec^{-1} . Note that all $\vec{\nabla}$ operators are in velocity space in this report. The diffusion current \vec{I} can be written as

$$\vec{I} = f\vec{A} - \vec{D} \cdot \vec{\nabla} f, \quad (2.4)$$

where \vec{A} and \vec{D} are the dynamical frictional and diffusion coefficients, respectively:

$$\vec{A}(\vec{v}) = - \frac{4\pi e^4 \ln \Lambda}{m^2} \int f(\vec{v}') \frac{(\vec{v} - \vec{v}')}{|\vec{v} - \vec{v}'|^3} d^3 v' \quad (2.5)$$

$$\vec{D}(\vec{v}) = \frac{2\pi e^4 \ln \Lambda}{m^2} \vec{\nabla} \cdot \vec{\nabla} \int f(\vec{v}') |\vec{v} - \vec{v}'| d^3 v'. \quad (2.6)$$

For simplicity, we consider only ion-ion collisions. The boundary condition to be satisfied by f is that it match the distribution function of the passing ions on the trapped-passing boundary in Fig. 1. The passing ion distribution function is taken to be a Maxwellian under the assumption that the central cell is long compared with the thermal barrier. The trapped ion distribution

function is symmetric in v_{\parallel} and has its dominant part in the neighborhood of the trapped-passing boundary in a well-pumped thermal barrier.

In order to match the real boundary shape and the value of f on the boundary we assume a separable form for the trapped ion distribution function $f(\vec{v})$,

$$f(\vec{v}) = R(v_1)Z(\eta) \quad (2.7)$$

where \vec{v}_1 is the vector from the vertex of the boundary hyperbola to a field point \vec{v} (see Fig. 3)

$$\vec{v}_1 = \vec{v} - \vec{v}_b . \quad (2.8)$$

Here \vec{v}_b is the vector from the origin to the vertex of the boundary hyperbola. η is a second velocity space variable to be determined later. The surface $\eta = 0$ is defined to be the trapped-passing boundary. We define $Z(\eta = 0) = 1$. The boundary condition on f is that it match the Maxwellian distribution of the passing particles; this becomes a constraint on the choice of R , which is taken to be only a function of v_1 , the magnitude of \vec{v}_1 . On the boundary, we need

$$R = G e^{-mv^2/2T_p} e^{\phi_b/T_p} \quad (2.9)$$

where G is a normalization constant determined by the passing ion density, n_p , in the thermal barrier,

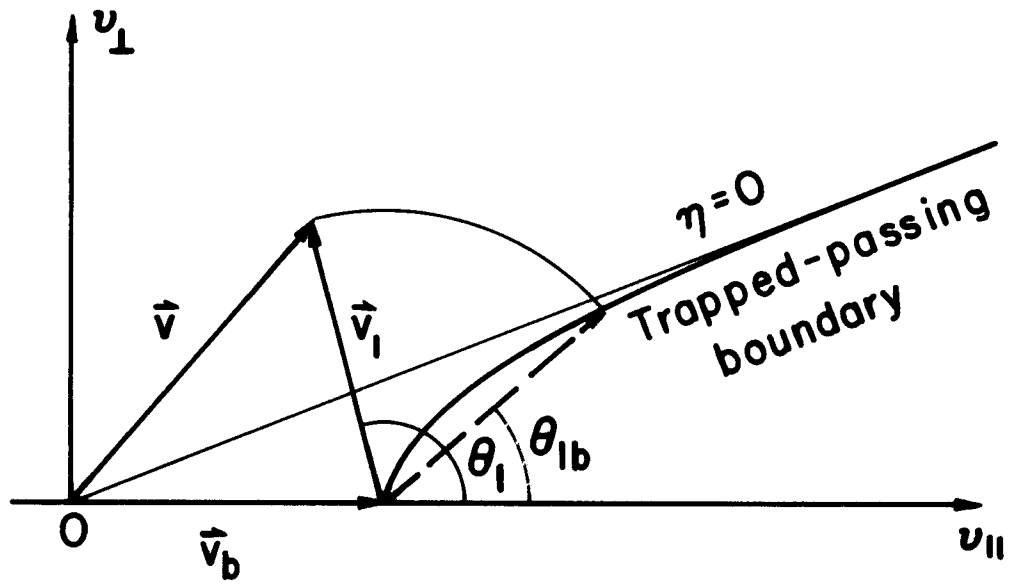


Fig. 3 The center-shifted coordinate system $(v_{\perp}, \theta_{\perp}, \psi)$ in velocity space.

$$G = \left(\frac{n_p}{H}\right) \left(\frac{m}{2\pi T_p}\right)^{3/2} \quad (2.10)$$

where

$$H = \exp\left(\frac{\phi_b}{T_p}\right) \operatorname{erfc}\left(\sqrt{\frac{\phi_b}{T_p}}\right) - \sqrt{1 - \frac{1}{R_b}} \exp\left(\frac{\phi_b}{T_p} \frac{R_b}{(R_b - 1)}\right) \operatorname{erfc}\left(\sqrt{\frac{\phi_b}{T_p} \frac{R_b}{(R_b - 1)}}\right) . \quad (2.11)$$

For large ϕ_b , R_b ,

$$H \approx \frac{1}{R_b} \sqrt{\frac{T_p}{\pi \phi_b}} .$$

The desired expression for R is obtained by letting

$$v^2 = (\vec{v}_1 + \vec{v}_b)^2 = v_1^2 + v_b^2 + 2v_1 v_b \cos \theta_1$$

and replacing θ_1 by θ_{1b} , the value of θ_1 on the boundary. One gets

$$R(v_1) = G e^{-mv_1^2/2T_p} e^{-mv_1 v_b \cos \theta_{1b}/T_p} \quad (2.12)$$

where

$$\cos \theta_{1b} = \frac{1}{R_b} \left[-\frac{v_b}{v_1} + \sqrt{\left(\frac{v_b}{v_1}\right)^2 + R_b(R_b - 1)} \right] . \quad (2.13)$$

Substituting Eqs. (2.7) and (2.4) into Eq. (2.3), we get

$$-\vec{\nabla} \cdot [Z(\vec{R}\vec{A} - \vec{D} \cdot \vec{\nabla} R)] + \vec{\nabla} \cdot [R\vec{D} \cdot \vec{\nabla} Z] - vRZ = 0 , \quad (2.14)$$

which is an equation determining Z. In the expressions for \vec{A} and \vec{D} (Eq. (2.5) and (2.6)) we replace the distribution function f by R(v_1) and integrate only

over the $v_{\parallel} > 0$ half (including the passing ions) of the phase space. The justification for this latter assumption is that the relative velocity is smaller for trapped particles having the same sign for v_{\parallel} and hence this should be the dominant contribution. Consequently, we can consider only the $v_{\parallel} > 0$ half-space with passing ion density, $n_p/2$, and total ion density, $n_b/2$. We compute the transport coefficients and trapping current ignoring the $v_{\parallel} < 0$ half-space and double the result in the end to get the total trapping current. We renormalize the transport coefficients to half the total ion density, $n_b/2$, in the barrier. Hence, replacing f by $R(v_1)$ in \vec{A} and \vec{D} affects only the isotropy of the field particle distribution function and not the total field particle density, n_b . Since \vec{A} and \vec{D} no longer depend on Z , Eq. (2.14) has been linearized by this assumption. This allows us to construct a variational principle from Eq. (2.14).

We define

$$\vec{\epsilon} = R\vec{A} - \vec{D} \cdot \vec{\nabla} R . \quad (2.15)$$

The vector $\vec{\epsilon}$ is, in general, non-zero since $R(v_1)$ is not Maxwellian, even centered around $\vec{v}_1 = 0$. Since \vec{A} and \vec{D} are isotropic about $\vec{v}_1 = 0$, we can write

$$\vec{\epsilon} = t\vec{v}_1$$

so that Eq. (2.14) becomes

$$\vec{\nabla} \cdot (R\vec{D} \cdot \vec{\nabla} Z) - vRZ - \vec{\nabla} \cdot (\vec{\epsilon} Z) = 0 . \quad (2.16)$$

Since Z depends only on n , one can integrate Eq. (2.16) over v_1 and the azimuthal angle ψ to get an ordinary differential equation for $Z(n)$. We use a generalization of Gauss' theorem (see Appendix I)

$$\iint dv_1 d\psi J(v_1, n) \vec{\nabla} \cdot \vec{C} = \frac{d}{dn} [\iint dv_1 d\psi J(v_1, n) \vec{\nabla} n \cdot \vec{C}] \quad (2.17)$$

where $J(v_1, n)$ is the Jacobian

$$J(v_1, n) = \frac{\partial(v_1, \theta, \psi)}{\partial(v_1, n, \psi)} = v_1^2 \sin \theta_1 \left. \frac{\partial \theta_1}{\partial n} \right|_{v_1, \psi} . \quad (2.18)$$

Using (2.17), we get

$$\frac{d}{dn} [p(n) \frac{dZ}{dn}] - q_0(n)Z - \frac{d}{dn} [q_1(n)Z] = 0 \quad (2.19)$$

where

$$p(n) = \iint dv_1 d\psi J(v_1, n) \vec{\nabla} n \cdot R \vec{D} \cdot \vec{\nabla} n \quad (2.20)$$

$$q_0(n) = \iint dv_1 d\psi J(v_1, n) vR \quad (2.21)$$

$$q_1(n) = \iint dv_1 d\psi J(v_1, n) \vec{t} \cdot \vec{\nabla} n . \quad (2.22)$$

The $q_1(n)$ term in Eq. (2.19) is dropped in order to put the equation in Sturm-Liouville form. This can be justified by noting that \vec{t} is small and that \vec{t} is approximately parallel to the boundary. By comparing Eq. (2.15) with Eq. (2.4), we see that \vec{t} is the diffusion current associated with a distribution function equal to R . Since the f inside \vec{A} and \vec{D} is replaced by R , \vec{t} would be zero if R were a true Maxwellian centered about $\vec{v}_1 = 0$. In our

case R is given by Eq. (2.12) which is not far from a center-shifted Maxwellian. Consequently, we expect $\vec{\epsilon}$ to be small. In addition, $\vec{\epsilon}$ is parallel to \vec{v}_1 , which is approximately parallel to the boundary (see Fig. 3).

Hence we take

$$\frac{d}{d\eta} \left[p(\eta) \frac{dZ}{d\eta} \right] - q_0(\eta)Z = 0 . \quad (2.23)$$

3. The Variational Functional

The variational functional that we choose is

$$L(Z) = \int d\eta \left\{ p(\eta) \left(\frac{dZ}{d\eta} \right)^2 + q_0(\eta) Z^2(\eta) \right\} , \quad (3.1)$$

where the η integration is only over the $v_{\parallel} > 0$ half-space. This is a standard form; it can easily be shown that $L(Z)$ is stationary for functions Z satisfying Eq. (2.23). This $L(Z)$ has a physical meaning. First we calculate the rate at which ions become trapped in the thermal barrier

$$J_{\text{trap}} = \int \vec{I} \cdot d\vec{S} = -2 \int dv_1 d\psi J(\eta, v_1) \vec{\nabla}_\eta \cdot (Z t \vec{v}_1 - R \vec{D} \cdot \vec{\nabla} Z) \Big|_{\eta=0}^{\eta=\eta_1} , \quad (3.2)$$

where η_1 is the value of η on the midplane ($v_{\parallel} = 0$). The v_1 integration is only for the $v_{\parallel} > 0$ half-space. The factor 2 comes from considering that there is also a similar trapped-passing boundary for $v_{\parallel} < 0$. In a well-pumped thermal barrier, there are few trapped particles on the midplane ($v_{\parallel} = 0$) so that we can write

$$J_{\text{trap}} \cong 2 \int dv_1 d\psi J(\eta, v_1) \vec{\nabla}_\eta \cdot (Z t \vec{v}_1 - R \vec{D} \cdot \vec{\nabla} Z) \Big|_{\eta=0} .$$

Using Eq. (2.20) and neglecting the $\nabla_{\eta} \cdot \mathbf{t} \mathbf{v}_1$ term, which is consistent with our previous approximation, we get

$$J_{\text{trap}} \cong -2p(\eta) \left. \frac{dZ}{d\eta} \right|_{\eta=0} . \quad (3.3)$$

We return to Eq. (3.1) and Eq. (2.23) to evaluate $L(Z)$ at its stationary value,

$$\begin{aligned} L(Z) \Big|_{\text{st.}} &= \int d\eta \left\{ p(\eta) \left(\frac{dZ}{d\eta} \right)^2 + Z(\eta) \frac{d}{d\eta} \left(p(\eta) \frac{dZ}{d\eta} \right) \right\} \\ &= \int d\eta \frac{d}{d\eta} \left(p(\eta) Z(\eta) \frac{dZ}{d\eta} \right) \\ &= p(\eta) Z(\eta) \left. \frac{dZ}{d\eta} \right|_{\eta=0}^{\eta=\eta_1} \\ &= -p(\eta) \left. \frac{dZ}{d\eta} \right|_{\eta=0} \end{aligned} \quad (3.4)$$

since $Z(\eta=0) = 1$ and little contribution comes from $\eta = \eta_1$. Comparing (3.3) and (3.4), we get

$$J_{\text{trap}} = 2L(Z) \Big|_{\text{stationary}} \quad (3.5)$$

within the context of our approximations. Consequently, the stationary value of the variational functional gives us the trapping current directly.

We still need to choose the coordinate η . To do this, we consider the simplified case where $R(v_1)$ is replaced by a center-shifted Maxwellian

$$R(v_1) \rightarrow R^M(v_1) = G \exp(-mv_1^2/2T_p) . \quad (3.6)$$

$$\text{Then, from Eq. (2.15)} \quad \vec{t} = 0 \quad (3.7)$$

where \vec{A} and \vec{D} are replaced by their Maxwellian versions \vec{A}^M and \vec{D}^M , respectively. Equation (2.16) in the (v_1, θ_1) coordinate system becomes

$$\frac{1}{v_1^2} \frac{\partial}{\partial v_1} (v_1^2 R^M D_{\parallel}^M \hat{e}_v \cdot \vec{\nabla} Z) + \frac{1}{v_1 \sin \theta_1} \frac{\partial}{\partial \theta_1} (\sin \theta_1 R^M D_{\perp}^M \hat{e}_{\theta} \cdot \vec{\nabla} Z) - v R^M(v_1) Z = 0 , \quad (3.8)$$

where $\hat{e}_v, \hat{e}_{\theta}$ are unit vectors in the \vec{v}_1 and θ_1 directions, respectively. We use the approximation

$$\hat{e}_v \cdot \vec{\nabla} Z \Big|_{\text{boundary}} \approx 0 \quad (3.9)$$

as discussed earlier, and

$$\hat{e}_{\theta} \cdot \vec{\nabla} Z \approx \frac{1}{v_1} \frac{\partial Z}{\partial \theta_1}$$

to put Eq. (3.8) in the form

$$\begin{aligned} & \frac{R^M D_{\perp}^M}{v_1^2 \sin \theta_1} \frac{\partial}{\partial \theta_1} \left(\sin \theta_1 \frac{\partial Z}{\partial \theta_1} \right) = v R^M Z , \\ \text{or} \quad & \frac{\partial^2 Z}{\partial \theta_1^2} + \cot \theta_1 \frac{\partial Z}{\partial \theta_1} - \frac{v v_1^2}{D_{\perp}^M} Z = 0 . \end{aligned} \quad (3.10)$$

It is difficult to find an exact analytical solution for Eq. (3.10). But for the most important region -- near the boundary surface and close to the tip of

the boundary -- the second term in Eq. (3.10) is very small. We can write down the solution for Eq. (3.10) without the second term,

$$Z(\theta_1) = C \exp\left(\pm \sqrt{\frac{\nu v_1^2}{D_\perp^M}} \theta_1\right) .$$

Using the boundary condition, $Z(\theta_{1b}) = 1$, and taking the decaying solution, we have

$$Z(\theta_1) = \exp\left(-\sqrt{\frac{\nu v_1^2}{D_\perp^M}} (\theta_1 - \theta_{1b})\right) .$$

In order to include the second term in Eq. (3.10), we use the form

$$Z(\theta_1) = \exp(S(\theta_1)) . \quad (3.11)$$

In the vicinity of the boundary, we may expand $S(\theta_1)$ as a power series of $(\theta_1 - \theta_{1b})$,

$$S(\theta_1) = S_0 + S_1(\theta_1 - \theta_{1b}) + S_2(\theta_1 - \theta_{1b})^2 + \dots . \quad (3.12)$$

Substituting (3.11) and (3.12) into Eq. (3.10) and using the boundary conditions, we can fix these coefficients,

$$S_0 = 0$$

$$S_1 = -\sqrt{\frac{\nu v_1^2}{D_\perp^M}}$$

$$S_2 = + \frac{1}{2} \sqrt{\frac{v v_1^2}{D_{\perp}^M}} \cot \theta_{1b} .$$

Consequently approximate analytical solution of Eq. (3.10) in the vicinity of the boundary is

$$Z(\theta_1) = \exp\left\{-\sqrt{\frac{v v_1^2}{D_{\perp}^M}} (\theta_1 - \theta_{1b}) \left[1 - \frac{1}{2} (\cot \theta_{1b}) (\theta_1 - \theta_{1b})\right]\right\} . \quad (3.12)$$

Based on this approximate solution for the simplified case, we take

$$\eta = \sqrt{\frac{v v_1^2}{D_{\perp}^M}} (\theta_1 - \theta_{1b}) \left[1 - \frac{1}{2} (\cot \theta_{1b}) (\theta_1 - \theta_{1b})\right] . \quad (3.13)$$

From Eq. (3.13) we get the shape of the contours of constant η . But we do not know the density of these contours, since the diffusion coefficient D_{\perp}^M is unknown. The Maxwellian version of the perpendicular diffusion coefficient D_{\perp}^M is defined as

$$D_{\perp}^M = \frac{2\pi e^4 n \Lambda}{m^2} \left(\frac{n^*}{2}\right) \frac{1}{v} \left[\phi(x) - \frac{\phi_1(x)}{2x^2}\right] .$$

$\phi(x)$ is the error function, $\text{erf}(x)$, and $x \equiv v_1/v_{th}$, with $v_{th} = \sqrt{2T/m}$. In the low velocity approximation

$$D_{\perp}^M \rightarrow \frac{2\pi e^4 n \Lambda}{m^2} \left(\frac{n^*}{2}\right) \frac{4}{3\sqrt{\pi}} v_{th} .$$

Since the field particles are a mixture of passing particles and trapped particles, we do not know their "effective temperature," therefore the thermal velocity v_{th} is unknown. At this stage, we also do not know the total density

$(n^*/2)$ so D_{\perp}^M is not yet defined. However, we know that D_{\perp}^M only affects the density of these contours of constant n , but not the shape of the contours. So we can introduce a variational parameter to take care of the density of these contours, and set any reasonable value for the field particle density and the effective temperature in the D_{\perp}^M . Hence we assume a trial function

$$Z(n) = \exp(-an) \quad (3.14)$$

where a is the variational parameter. Then, n is determined when the field particle density is assigned a value of $n_p/2$ and the effective temperature is assigned a value of T_p . Now the trial function $Z(n)$ borrows the shape of the contours from the simplified case (Eq. 3.10), and satisfies the real boundary condition ($Z(0) = 1$ at the trapped-passing boundary, $n = 0$). The density of the contours of constant $Z(n)$ is taken care of by the variational parameter a , which will be determined by the variational principle, that is, by the stationary condition

$$\frac{\partial L}{\partial a} = 0 \quad (3.15)$$

We now substitute the trial function $Z(n)$ from Eq. (3.14) into the functional $L(Z)$, Eq. (3.1), and choose a using Eq. (3.15). This becomes

$$2 \int_0^{n_1} dn e^{-2an} \{ap(n) - n[a^2p(n) + q_0(n)]\} = 0 \quad (3.16)$$

Because of the exponential factor in the integrand, $p(n)$ and $q_0(n)$ may be expanded in a Taylor series around $n = 0$. Hence we get

$$\int_0^{\eta_1} d\eta e^{-2a\eta} \left\{ a(1 - na) \left(p(0) + \eta \frac{dp}{d\eta} \Big|_0 \right) - n(q_0(0) + \eta \frac{dq_0}{d\eta} \Big|_{\eta=0}) \right\} = 0 .$$

The upper limit of this integration is a number η_1 which makes $z(\eta_1) \sim 0$. The dominant contribution comes from $\eta \approx 0$. After integration, we get

$$\frac{p(0)}{4} - \frac{q_0(0)}{4a^2} - \frac{1}{4a^3} \frac{dq_0}{d\eta} \Big|_{\eta=0} = 0 .$$

It is shown in Appendix II that $dq_0/d\eta|_{\eta=0} \approx 0$ so the solution for a is

$$a = \sqrt{\frac{q_0(0)}{p(0)}} . \quad (3.17)$$

Note, the $p(0)$ here involves the real diffusion tensor \vec{D} (see Eq. 2.20) which has both the D_{\parallel} component and the D_{\perp} component with the real density and effective temperature. So the variational parameter a expresses the effects of the total density, the effective temperature, and the D_{\parallel} component.

We insert the solution (3.17) for a back into the trial function, Eq. (3.14), and put this into $L(Z)$ to estimate the trapping current. We get

$$J_{\text{trap}} = ap(0) + \frac{q_0(0)}{a} + \frac{1}{2} \frac{dp}{d\eta} \Big|_{\eta=0} . \quad (3.18)$$

Using (3.17) and $dp/d\eta|_{\eta=0} \approx 0$ (see Appendix III), this becomes

$$J_{\text{trap}} = 2\sqrt{p(0)q_0(0)} . \quad (3.19)$$

4. The Total Ion Density

There is one remaining complication which we now consider. The diffusion tensor \tilde{D} , which is contained in $p(0)$ and therefore in a , depends on the total ion density, which has not yet been obtained. We integrate Eq. (2.3) over the trapped particle part of velocity space to get the trapping current,

$$J_{\text{trap}} = v n_t = v(n_b - n_p) \quad (4.1)$$

where n_t , n_p , and n_b are the trapped, passing, and total ion density in the barrier. Generally speaking, n_p is determined by the central cell parameters, and v by the barrier pump neutral beams. Consequently Eq. (4.1) is another relationship between the trapping current per unit volume, J_{trap} , and the ion density, n_b , both of which are determined by the collisional relaxation processes in the barrier. Upon combining Eq. (4.1) with (3.19), we have

$$\frac{1}{2} v(n_b - n_p) = \sqrt{p(0)q(0)} \quad (4.2)$$

Since $p(0)$ is proportional to n_b through \tilde{D} , and both $p(0)$ and $q(0)$ are proportional to n_p through R , we may define

$$\hat{q}_0(0) = \frac{q_0(0)}{v n_p} = \int d\psi \int dv_1 J(v_1, 0) \hat{R} \quad (4.3)$$

$$\hat{p}(0) = \frac{2p(0)}{n_p n_b} = \int d\psi \int dv_1 J(v_1, 0) \hat{v}_n \cdot \hat{R} \hat{\tilde{D}} \cdot \hat{v}_n \quad (4.4)$$

with $\hat{R} = R/n_p$ and $\hat{\tilde{D}}$ is defined later. The pumping parameter, g_b , is defined as

$$g_b = \frac{n_b}{n_p} . \quad (4.5)$$

We get a quadratic equation for $\sqrt{g_b}$

$$g_b - \sqrt{2\alpha g_b} - 1 = 0 \quad (4.6)$$

where

$$\alpha = \frac{\hat{q}_0(0)\hat{p}(0)}{\nu} n_p . \quad (4.7)$$

The solution is

$$g_b = 1 + \alpha(1 + \sqrt{1 + \frac{2}{\alpha}}) . \quad (4.8)$$

Combining Eq. (4.8) with (4.5) and (4.1) gives us the expression

$$J_{\text{trap}} = \nu n_p \alpha(1 + \sqrt{1 + \frac{2}{\alpha}}) . \quad (4.9)$$

The calculation of the trapping current is thus reduced to the calculation of α for a given pumping rate ν and passing ion density, n_p . The calculation of α also requires the potential ϕ_b , the mirror ratio R_b , and the temperature T_p of the passing ions.

The calculation of $\hat{p}(0)$ needed for α requires $\hat{\vec{D}}$. Now

$$\nabla \eta \cdot \hat{\vec{D}} \cdot \nabla \eta = \hat{D}_{\parallel} \left(\frac{\partial \eta}{\partial v_1} \right)^2 + \hat{D}_{\perp} \left(\frac{1}{v_1} \frac{\partial \eta}{\partial \theta_1} \right)^2 \quad (4.10)$$

where

$$\hat{D}_{\perp} = \frac{2\pi e^4 \ln \Lambda}{m^2} \frac{1}{v_1} \int_0^{v_1} dv' \, 4\pi (v')^2 \frac{1}{C_0} R(v'_1) \left(1 - \frac{(v'_1)^2}{3v_1^2} \right) \quad (4.11)$$

$$+ \int_{v_1}^{\infty} dv'_1 \, 4\pi v_1'^2 \frac{1}{C_0} R(v'_1) \frac{2}{3} \left(\frac{v_1}{v'_1} \right)$$

$$\hat{D}_{\parallel} = \frac{2\pi e^4 n \Lambda}{m^2} \frac{1}{v_1} \left[\int_0^{v_1} dv'_1 4\pi v'^1_1{}^2 \frac{1}{C_0} R(v'_1) \frac{2}{3} \left(\frac{v'_1}{v_1}\right)^2 + \int_{v_1}^{\infty} dv'_1 4\pi v'^1_1{}^2 \frac{1}{C_0} R(v'_1) \frac{2}{3} \left(\frac{v_1}{v'_1}\right)^2 \right]. \quad (4.12)$$

C_0 is the normalization coefficient

$$C_0 = \int_0^{\infty} dv'_1 4\pi v'^1_1{}^2 R(v'_1).$$

Using the expression for η , (3.13), we have

$$\left. \frac{d\eta}{dv_1} \right|_{\eta=0} = \sqrt{\frac{v}{D_{\perp}^M}} \cdot \frac{\text{ctg } \theta_{1b}}{1 + (v_1/v_b) \cos \theta_{1b}} \quad (4.13)$$

$$\left. \frac{\partial \eta}{\partial \theta_1} \right|_{\eta=0} = \sqrt{\frac{v}{D_{\perp}^M}} v_1. \quad (4.14)$$

Here D_{\perp}^M in (4.13) and (4.14) is the Maxwellian version of the diffusion tensor with the density $(n_p/2)$, i.e.

$$D_{\perp}^M = \frac{2\pi e^4 n \Lambda}{m^2} \frac{n_p}{2} \frac{1}{v_1} \left[\Phi(x) - \frac{1}{2x^2} \left(\Phi(x) - x \frac{d\Phi}{dx} \right) \right].$$

$x \equiv v_1/\sqrt{(2T_p)/m}$. The calculation of α can now be done numerically. A typical computation requires less than 0.1 sec on the CRAY computer.

5. The Numerical Results and Comparison to Fokker-Planck Calculations

The variational procedure developed in the previous section has been implemented and applied to 21 cases calculated by Futch and LoDestro. Their calculations are obtained using a numerical Fokker-Planck code in which the

Rosenbluth potentials are evaluated using the actual anisotropic field particle distribution function. Figures 4 and 5 show the comparison for the low and high mirror ratio cases. The agreement between the two methods is surprisingly good. For the low mirror ratio case (Fig. 4) the relative error is generally less than 5% except in one case where it is 9%. For the high mirror ratio case (Fig. 5), the relative error is generally less than 10%, except in one case where it is 16%. Since the error in the Fokker-Planck code results is about 7% due to the finite grid size, we see the advantage of the variational method.

It is important to note that the comparisons in Figs. 4 and 5 are based upon treating the passing ion density as input data, as discussed in Section 4. The total ion density is then calculated self-consistently. This is also the way the Fokker-Planck code operates. In Ref. 9, the comparison was made on the basis of the same total ion density, n_b , since this is what directly determines the collision frequency, and therefore the trapping rate, in the thermal barrier. Comparison on the basis of a given passing ion density is a more sensitive test, however, since one has to calculate both the total density and the trapping rate. There are two steps in the calculation; making the comparison on the basis of the same total ion density is an improper avoidance of the first step. One can also see this from Eq. (4.1). We can rewrite it in the form

$$J_{\text{trap}} = v n_b \left(1 - \frac{1}{g_b}\right). \quad (5.1)$$

In the limit of large g_b , J_{trap} is only weakly dependent on g_b and approaches $v n_b$ (which are simply input data in Ref. 9). For example, Futch and LoDestro

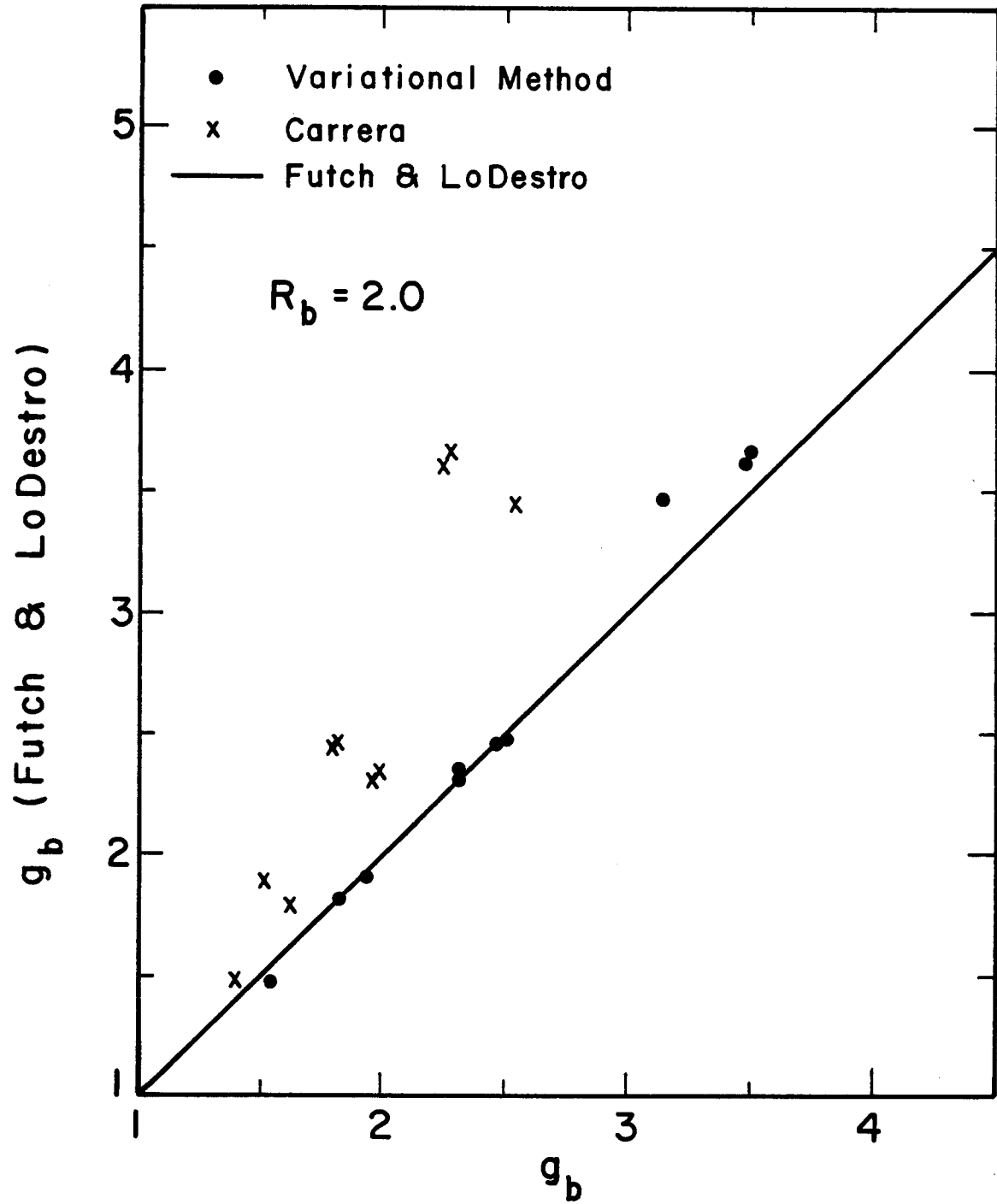


Fig. 4 Comparison of the trapping ratio, g_b , calculated by the three different methods (Low Mirror Ratio Cases; $R_b = 2$, $\phi_b = 40$ keV, $T_e = 15$ keV).

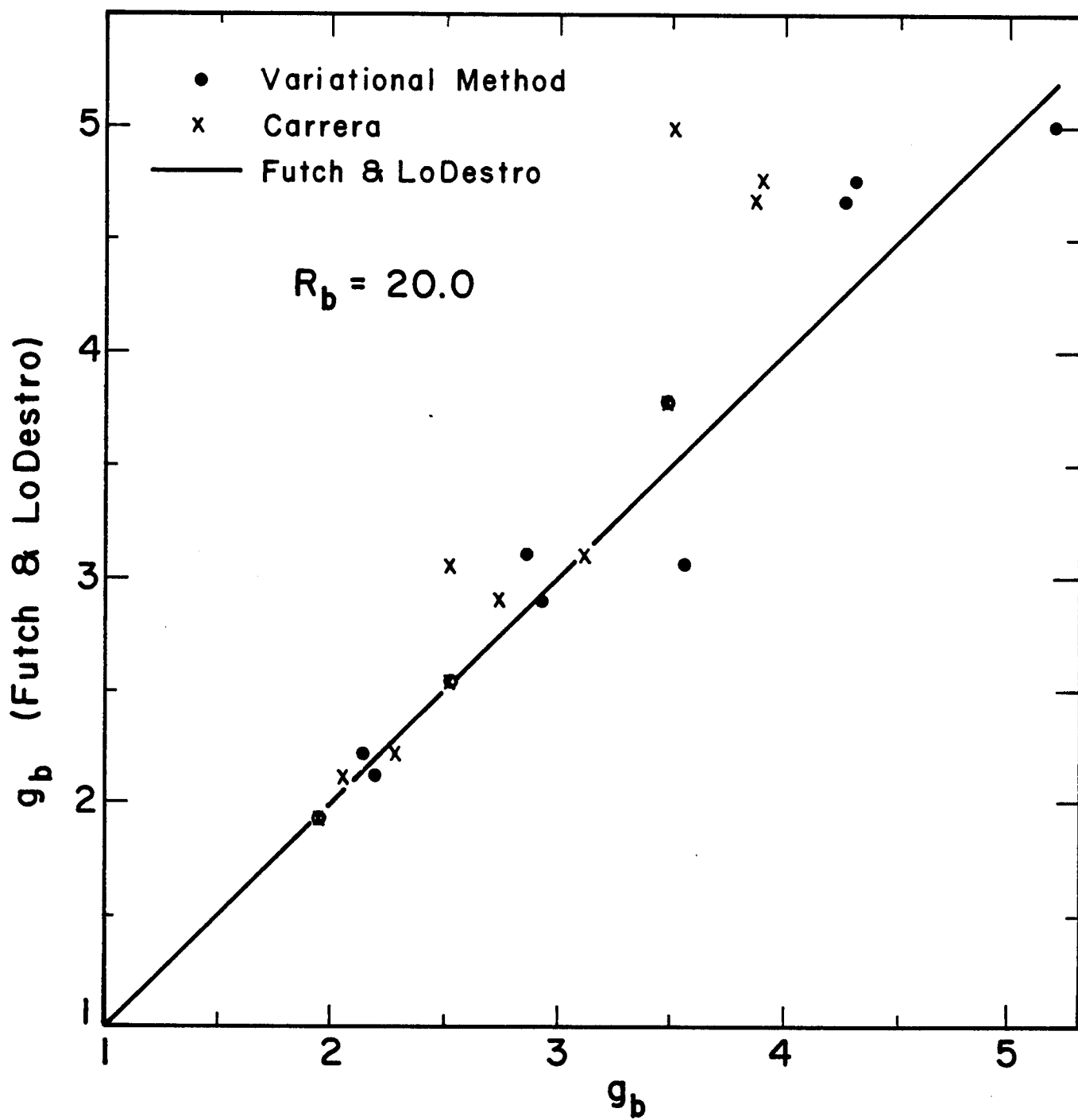


Fig. 5 Comparison of the trapping ratio, g_b , calculated by the three different methods (High Mirror Ratio Cases; $R_b = 20$, $\phi_b = 1$ keV, $T_e = 0.4$ keV).

used their code for the calculation of the low mirror ratio case ($R_b = 2$). They used the passing particle density, n_p , as input data to obtain the three output data: the total density in the barrier, n_b ; the trapping current, J_t ; and the ratio $g_b \equiv n_b/n_p$. With the input $n_p = 0.55 \times 10^{11} \text{ cm}^{-3}$, they obtained $n_b = 14.68 \times 10^{11} \text{ cm}^{-3}$, the trapping current $J_t = 3.53 \times 10^{11} \text{ cm}^{-3} \text{ sec}^{-1}$, and $g_b = 26.7$. Carrera used the code output value $n_b = 14.68 \times 10^{11} \text{ cm}^{-3}$ as his input and obtained his output $J_t = 3.09 \times 10^{11} \text{ cm}^{-3} \text{ sec}^{-1}$. This represents an error of 12% in J_t . However, one needs to compare the g_b value also. The corresponding g_b value implied by his calculation can be obtained by putting n_b and the calculated J_{trap} into Eq. (5.1). The result is $g_b = 6.32$, which compares poorly with the Fokker-Planck code result of 26.7. In fact, if we only need an estimate for the trapping current J_t using the total density, n_b , as input, we could simply use the formula,

$$J_t = v n_b \left(1 - \frac{1}{10}\right) = 0.9 v n_b$$

which has an error less than 13% as long as the real g_b is greater than 5. It can be seen from Eq. (5.1) that, when n_b is used as input,

$$\frac{\Delta J_t}{J_t} \approx \frac{\Delta g_b}{g_b^2} = \frac{1}{g_b} \left(\frac{\Delta g_b}{g_b}\right).$$

Consequently, the error in J_t is reduced by a factor of g_b from the error in g_b .

For a true test of the model, one should check g_b instead of J_t in the comparison with the code results. Consequently, in our comparison, we include

g_b . In addition, we use n_p as the input density since this also gives a more sensitive comparison. Our output is then n_b , J_t , and g_b .

Shown in Tables I and II are the input and output data for the code results,⁽⁸⁾ our variational method, and the analytical method of Ref. 9. To obtain the results for the analytical method of Ref. 9 but with n_p as input data, the basic equations of Ref. 9 were inverted to give J_{trap} , n_b and g_b , for a given n_p . The density n_b is gotten simply from $n_b = g_b n_p$ and thus is not shown in the tables. Case 27 of Ref. 8 is not included since, with such a large g_b , both the variational and analytical results are suspect.

The comparison in Tables I and II shows that both the analytical and variational methods give reasonable results in the high mirror ratio case. In the low mirror ratio case the variational method is more accurate, especially in calculating g_b . The analytical method has the advantage of simplicity, however. One merely needs to evaluate a closed form expression, whereas the variational method requires numerical evaluation of integrals. Both methods fail when g_b is large.

6. Discussion

A basic assumption of this calculation is that the two counter-streaming groups of particles in the thermal barrier do not interact very much with those streaming in the opposite direction if the barrier potential is greater than the temperature of the passing ions. Because of the velocity dependence of the Coulomb collision frequency, the dominant collisional interaction is with particles in the same group. In particular, the diffusion current across the trapped-passing boundary is determined mainly by collisions with particles near the boundary. Consequently, considerable effort was devoted to matching

TABLE I. Low Mirror Ratio Case

$R_b = 2$, $\phi_b = 40$ keV , $T_e = 15$ keV

Input Data			g _b		J _t (10 ¹¹ cm ⁻³ -sec ⁻¹)			
n _p (10 ¹¹ cm ⁻³)	T _p (keV)	ν (sec ⁻¹)	Numerical*	Variational Analytical**	Numerical*	Variational Analytical**		
1.1	15.0	0.25	3.45	3.14	2.54	0.675	0.589	0.424
1.1	15.0	0.5	2.31	2.30	1.96	0.721	0.715	0.528
1.1	15.0	1.0	1.80	1.82	1.62	0.880	0.902	0.682
1.1	15.0	2.0	1.48	1.53	1.41	1.06	1.17	0.902
0.55	15.0	0.25	2.33	2.31	1.97	0.183	0.180	0.133
1.1	10.0	0.5	3.62	3.48	2.25	1.44	1.36	0.688
1.1	10.0	1.0	2.46	2.49	1.79	1.61	1.64	0.869
1.1	10.0	2.0	1.90	1.93	1.52	1.98	2.05	1.14
0.55	10.0	0.25	3.66	3.50	2.27	0.366	0.344	0.175
2.2	10.0	2.0	2.45	2.47	1.79	6.38	6.47	3.48

* Ref. 8.

** Calculated using the analytical method of Ref. 9 as described in the text.

TABLE II. High Mirror Ratio Case

$R_b = 20$, $\phi_b = 1.0$ keV , $T_e = 0.4$ keV

Input Data			g_b		J_t ($10^{15} \text{ cm}^{-3}\text{-sec}^{-1}$)			
n_p (10^{11}cm^{-3})	T_p (keV)	ν (10^3sec^{-1})	Numerical* Variational Analytical**		Numerical* Variational Analytical**			
8.9	1/3	2.0	4.76	4.33	3.90	6.69	5.87	5.16
8.9	1/3	4.0	2.90	2.96	2.73	6.79	6.91	6.16
8.9	1/3	8.0	2.12	2.19	2.07	7.97	8.47	7.62
8.9	0.2	4.0	5.0	5.38	3.51	14.2	14.9	8.94
8.9	0.4	4.0	2.54	2.53	2.52	5.48	5.41	5.41
8.9	0.5	4.0	2.22	2.16	2.30	4.34	4.09	4.63
17.8	1/3	4.0	4.68	4.29	3.86	26.2	23.1	20.4
4.45	0.2	4.0	3.06	3.55	2.53	3.66	4.54	2.72
17.8	0.4	4.0	3.79	3.52	3.48	19.8	17.7	17.7
4.45	0.4	4.0	1.94	1.96	1.96	1.67	1.71	1.71
17.8	0.5	4.0	3.10	2.86	3.11	15.0	13.2	15.0

* Ref. 8.

** Calculated using the analytical method of Ref. 9 as described in the text.

the boundary condition as accurately as possible and maintaining the accuracy of the approximate solution in the vicinity of the boundary.

Energy diffusion plays an important role in the trapping process, particularly for the case of low mirror ratio (see Fig. 4). Since most of the particles are concentrated near the tip of the boundary, drag on passing particles will cause trapping. Pitch angle scattering, however, contributes little to trapping since the direction of pitch angle scattering (in the laboratory frame of reference) is almost parallel to the boundary. Shifting the pitch angle scattering "center" from $\vec{v} = 0$ to $\vec{v} = \vec{v}_b$ causes pitch angle scattering to be more normal to the trapped-passing boundary and produces a diffusion current across the boundary. Consequently, pitch angle scattering in the co-moving frame ($\vec{v} = \vec{v}_b$) is, in some sense, equivalent to energy diffusion in the laboratory frame.

The isotropic Rosenbluth potential approximation appears reasonable as long as the center is shifted to the tip of the boundary. In this frame of reference, the anisotropy is, in fact, reduced. Since the Rosenbluth potentials involve integrals over velocity space, anisotropy plays a small role in the calculation of \vec{D} and \vec{A} ; the anisotropy retained in our calculation is in $Z(\eta)$, which is important in determining the diffusion current. The agreement between our results and the numerical results of Futch and LoDestro is also "a posteriori" justification of our approximation.

More work is required before a true analytic result can be obtained. The integrals in $\hat{q}_0(0)$ and $\hat{p}(0)$ should be obtained analytically. Also the shape of the magnetic field and electrostatic potential, rather than using the square well approximation, should be taken into account for a better description of the trapping process in a real experiment.

Appendix I
A Generalized Gauss' Theorem

In any coordinate system, we have Gauss' Theorem

$$\iiint d^3\mathbf{v} \nabla \cdot \vec{\mathbf{C}} \equiv \iint d\vec{\mathbf{S}} \cdot \vec{\mathbf{C}} . \quad (\text{I.1})$$

Using the coordinate system $(\mathbf{v}_1, \eta, \psi)$ with the Jacobian J , we obtain

$$\iiint d^3\mathbf{v} \nabla \cdot \vec{\mathbf{C}} = \iiint d\eta d\mathbf{v}_1 d\psi J \nabla \cdot \vec{\mathbf{C}} . \quad (\text{I.2})$$

For the vector set $(\nabla \mathbf{v}_1, \nabla \eta, \nabla \psi)$ there is a reciprocal vector set $(\frac{\partial \vec{\mathbf{v}}}{\partial \mathbf{v}_1}, \frac{\partial \vec{\mathbf{v}}}{\partial \eta}, \frac{\partial \vec{\mathbf{v}}}{\partial \psi})$; therefore

$$\nabla \eta = \left(\frac{\partial \vec{\mathbf{v}}}{\partial \psi} \right) \times \left(\frac{\partial \vec{\mathbf{v}}}{\partial \mathbf{v}_1} \right) / \left[\left(\frac{\partial \vec{\mathbf{v}}}{\partial \psi} \right) \times \left(\frac{\partial \vec{\mathbf{v}}}{\partial \mathbf{v}_1} \right) \cdot \left(\frac{\partial \vec{\mathbf{v}}}{\partial \eta} \right) \right] . \quad (\text{I.3})$$

However, the Jacobian J can be defined as

$$J = \left(\frac{\partial \vec{\mathbf{v}}}{\partial \psi} \right) \times \left(\frac{\partial \vec{\mathbf{v}}}{\partial \mathbf{v}_1} \right) \cdot \left(\frac{\partial \vec{\mathbf{v}}}{\partial \eta} \right) . \quad (\text{I.4})$$

Hence,
$$\left(\frac{\partial \vec{\mathbf{v}}}{\partial \psi} \right) \times \left(\frac{\partial \vec{\mathbf{v}}}{\partial \mathbf{v}_1} \right) = J \nabla \eta . \quad (\text{I.5})$$

Since the differential surface element at constant η can be written as

$$d\vec{\mathbf{S}} = \left(\frac{\partial \vec{\mathbf{v}}}{\partial \psi} \right) \times \left(\frac{\partial \vec{\mathbf{v}}}{\partial \mathbf{v}_1} \right) d\psi d\mathbf{v}_1 , \quad (\text{I.6})$$

we have
$$\iint d\vec{S} \cdot \vec{C} = \iint \left(\frac{\partial \vec{v}}{\partial \psi} \right) \times \left(\frac{\partial \vec{v}}{\partial v_1} \right) dv_1 d\psi \cdot \vec{C} = \iint dv_1 d\psi J \nabla \eta \cdot \vec{C} . \quad (I.7)$$

Substituting Eqs. (I.2) and (I.6) into Eq. (I.1), we have

$$\iiint d\eta dv_1 d\psi J \nabla \cdot \vec{C} = \iint dv_1 d\psi J \nabla \eta \cdot \vec{C} . \quad (I.8)$$

Taking the derivative with respect to η on both sides of Eq. (I.8), we have our desired result,

$$\iint dv_1 d\psi J \nabla \cdot \vec{C} = \frac{d}{d\eta} \iint dv_1 d\psi J \nabla \eta \cdot \vec{C} . \quad (I.9)$$

Appendix II
The Calculation of $\frac{dq}{d\eta}\big|_{\eta=0}$

We have

$$q_0(\eta) \equiv 2\pi \int_{v_{\min}}^{\infty} dv_1 J(v_1, \eta) vR(v_1) . \quad (II.1)$$

The lower limit of the integration, v_{\min} , is not zero when η is nonzero, since v_1 is the distance from the tip of the $\eta = 0$ surface to any point on the $\eta = \text{constant}$ surface. Now

$$\frac{d}{d\eta} q_0(\eta) = -2\pi J(v_{\min}, \eta) vR(v_{\min}) \cdot \frac{dv_{\min}}{d\eta} + 2\pi \int_{v_{\min}}^{\infty} dv_1 vR(v_1) \frac{\partial}{\partial \eta} J(v_1, \eta) . \quad (II.2)$$

Since

$$J(v_1, \eta) = v_1^2 \sin \theta_1 \frac{1}{\left(\frac{\partial \eta}{\partial \theta_1}\right)} \quad (II.3)$$

and

$$\theta_1(v_{\min}, \eta) = \pi$$

we have

$$J(v_{\min}, \eta) = 0 . \quad (II.4)$$

For the second term in Eq. (II.2), we use

$$\begin{aligned} \frac{\partial}{\partial \eta} J(v_1, \eta) &= v_1^2 \frac{\partial}{\partial \eta} \left[\sin \theta_1 \frac{1}{\left(\frac{\partial \eta}{\partial \theta_1}\right)} \right] \\ &= v_1^2 \left[\cos \theta_1 \frac{\partial \theta_1}{\partial \eta} \frac{1}{\left(\frac{\partial \eta}{\partial \theta_1}\right)} + \sin \theta_1 \frac{(-1)}{\left(\frac{\partial \eta}{\partial \theta_1}\right)^2} \frac{\partial}{\partial \eta} \left(\frac{\partial \eta}{\partial \theta_1}\right) \right] . \end{aligned} \quad (II.5)$$

However,

$$\frac{\partial}{\partial \eta} \left(\frac{\partial \eta}{\partial \theta_1} \right) = \left(\frac{\partial^2 \eta}{\partial \theta_1^2} \right) \left(\frac{\partial \theta_1}{\partial \eta} \right) = \frac{1}{\left(\frac{\partial \eta}{\partial \theta_1} \right)} \left(\frac{\partial^2 \eta}{\partial \theta_1^2} \right) . \quad (II.6)$$

From Eq. (3.13), we have

$$\frac{\partial \eta}{\partial \theta_1} = + \sqrt{\frac{v v_1^2}{D_{\perp}^M}} [1 - (\cot \theta_{1b})(\theta_1 - \theta_{1b})] \quad (II.7)$$

$$\frac{\partial^2 \eta}{\partial \theta_1^2} = - \sqrt{\frac{v v_1^2}{D_{\perp}^M}} \cot \theta_{1b} . \quad (II.8)$$

Hence

$$\begin{aligned} \frac{\partial}{\partial \eta} J(v_1, \eta) &= v_1^2 \left[\cos \theta_1 \frac{1}{\left(\frac{\partial \eta}{\partial \theta_1} \right)^2} - \sin \theta_1 \frac{1}{\left(\frac{\partial \eta}{\partial \theta_1} \right)^2} \frac{(-\cot \theta_{1b})}{1 - \cot \theta_{1b}(\theta_1 - \theta_{1b})} \right] \\ &\underset{\theta_1 \rightarrow \theta_{1b}}{=} v_1^2 \frac{1}{\left(\frac{\partial \eta}{\partial \theta_1} \right)^2} [\cos \theta_1 + \sin \theta_1 \cot \theta_{1b}] \\ &\rightarrow v_1^2 \frac{1}{\left(\frac{\partial \eta}{\partial \theta_1} \right)^2} 2 \cos \theta_{1b} = 2 \frac{J(v_1, 0) \cot \theta_{1b}}{\left(\frac{\partial \eta}{\partial \theta_1} \right)} . \end{aligned} \quad (II.9)$$

So

$$\left. \frac{d}{d\eta} q_0(\eta) \right|_{\eta=0} = 2\pi \int_0^{\infty} dv_1 J(v_1, 0) \frac{2 \cot \theta_{1b}}{\sqrt{\frac{v v_1^2}{D_{\perp}^M}}} v R(v_1) . \quad (II.10)$$

Since $R(v_1)$ is a dramatically descending function of v_1 , only small v_1 contributes to the integration. For the small v_1 , $\cos \theta_{1b} \rightarrow 0$. Therefore, $\left. \frac{d}{d\eta} q_0(\eta) \right|_{\eta \rightarrow 0}$ is negligible compared to $q_0(\eta \rightarrow 0)$.

Appendix III
The Calculation of $\left. \frac{dp}{d\eta} \right|_{\eta=0}$

The definition of $p(\eta)$ is

$$p(\eta) \equiv \iint dv_1 d\psi J \nabla \eta \cdot R \vec{D} \cdot \nabla \eta = 2\pi \int_{v_{\min}(\eta)}^{\infty} dv_1 J R \left[\left(\frac{1}{v_1} \frac{\partial \eta}{\partial \theta_1} \right)^2 D_{\perp} + \left(\frac{\partial \eta}{\partial v_1} \right)^2 D_{\parallel} \right].$$

The Jacobian J is

$$J = v_1^2 \sin \theta_1 \frac{1}{\left(\frac{\partial \eta}{\partial \theta_1} \right)}.$$

η can be written as

$$\eta \equiv \xi(v_1) \left[1 - \frac{1}{2} \cot \theta_{1b} (\theta_1 - \theta_{1b}) \right] (\theta_1 - \theta_{1b})$$

where $\xi(v_1) \equiv \sqrt{\frac{v v_1^2}{D_{\perp}^M}}$ is a function of only v_1 , and $v_{\min}(\eta)$ is the value of v_1

when $\theta_1 = \pi$. We calculate all the derivatives as follows:

$$\frac{\partial \eta}{\partial \theta_1} = \xi(v_1) [1 - \cot \theta_{1b} (\theta_1 - \theta_{1b})] \rightarrow \xi(v_1) \quad \text{as } \theta_1 \rightarrow \theta_{1b}$$

$$\begin{aligned} \frac{\partial \eta}{\partial v_1} &= \left(\frac{\partial \xi}{\partial v_1} \right) \left[1 - \frac{1}{2} \cot \theta_{1b} (\theta_1 - \theta_{1b}) \right] (\theta_1 - \theta_{1b}) \\ &\quad + \xi(v_1) \left[-\frac{\partial \theta_{1b}}{\partial v_1} + \frac{1}{2} \cot \theta_{1b} \cdot 2(\theta_1 - \theta_{1b}) \left(\frac{\partial \theta_{1b}}{\partial v_1} \right) \right. \\ &\quad \left. - \frac{1}{2} \frac{-1}{\sin^2 \theta_{1b}} (\theta_1 - \theta_{1b})^2 \left(\frac{\partial \theta_{1b}}{\partial v_1} \right) \right] \rightarrow \xi(v_1) \left(-\frac{\partial \theta_{1b}}{\partial v_1} \right) \quad \text{as } \theta_1 \rightarrow \theta_{1b} \end{aligned}$$

θ_{1b} is defined as

$$\cos \theta_{1b} = \frac{1}{R_b} \left[-\left(\frac{v_b}{v_1}\right) + \sqrt{\left(\frac{v_b}{v_1}\right)^2 + R_b(R_b - 1)} \right] .$$

Hence,

$$-\sin \theta_{1b} \frac{\partial \theta_{1b}}{\partial v_1} = \frac{1}{R_b} \left[\frac{v_b}{v_1^2} + \frac{\frac{v_b^2}{v_1} \left(-\frac{1}{v_1^2}\right)}{\sqrt{\left(\frac{v_b}{v_1}\right)^2 + R_b(R_b - 1)}} \right] .$$

We obtain the result

$$\frac{\partial \theta_{1b}}{\partial v_1} = -\frac{1}{v_1} \cot \theta_{1b} \frac{1}{1 + \frac{v_1}{v_b} R_b \cos \theta_{1b}} .$$

Therefore

$$\begin{aligned} \frac{dp}{dn} = & 2\pi \int_{v_{\min}(n)}^{\infty} dv_1 \frac{\partial J}{\partial n} R \left[\left(\frac{1}{v_1} \frac{\partial n}{\partial \theta_1} \right)^2 D_{\perp} + \left(\frac{\partial n}{\partial v_1} \right)^2 D_{\parallel} \right] \\ & + 2\pi \int_{v_{\min}(n)}^{\infty} dv_1 J R \left[2 \left(\frac{1}{v_1} \frac{\partial n}{\partial \theta_1} \right) \frac{\partial}{\partial n} \left(\frac{1}{v_1} \frac{\partial n}{\partial \theta_1} \right) D_{\perp} + 2 \left(\frac{\partial n}{\partial v_1} \right) \frac{\partial}{\partial n} \left(\frac{\partial n}{\partial v_1} \right) D_{\parallel} \right] \\ & + 2\pi(-1)JR \left[\left(\frac{1}{v_1} \frac{\partial n}{\partial \theta_1} \right)^2 D_{\perp} + \left(\frac{\partial n}{\partial v_1} \right)^2 D_{\parallel} \right] \frac{\partial v_{\min}(n)}{\partial n} \Big|_{v_1=v_{\min}(n)} . \end{aligned}$$

When

$$n \rightarrow 0, v_{\min}(n) \rightarrow 0$$

and

$$J \Big|_{v_{\min}(\eta)} \Big|_{\eta \rightarrow 0} = v_1^2 \sin \theta_1 \frac{1}{\left(\frac{\partial \eta}{\partial \theta_1}\right)} \Big|_{v_1 \rightarrow 0, \theta_1 \rightarrow \pi}$$

$$\propto v_1^2 \sin \theta_1 \frac{1}{v_1} \rightarrow 0 .$$

Hence the third term in $\frac{dp}{d\eta} \Big|_{\eta=0}$ vanishes. Now we show that the terms involving D_{\perp} cancel each other. Since

$$\frac{\partial J}{\partial \eta} = v_1^2 \cos \theta_1 \frac{\partial \theta_1}{\partial \eta} \frac{1}{\frac{\partial \eta}{\partial \theta_1}} + v_1^2 \sin \theta_1 \frac{-1}{\left(\frac{\partial \eta}{\partial \theta_1}\right)^2} \frac{\partial}{\partial \eta} \left(\frac{\partial \eta}{\partial \theta_1}\right)$$

$$= v_1^2 \frac{1}{\left(\frac{\partial \eta}{\partial \theta_1}\right)^2} [\cos \theta_1 - \sin \theta_1 \frac{\partial}{\partial \eta} \left(\frac{\partial \eta}{\partial \theta_1}\right)]$$

and

$$\frac{\partial}{\partial \eta} \left(\frac{\partial \eta}{\partial \theta_1}\right) = \xi(v_1)(-\cot \theta_{1b}) \left(\frac{\partial \theta_1}{\partial \eta}\right)$$

$$= \xi(v_1)(-\cot \theta_{1b}) \frac{1}{\xi(v_1)[1 - \cot \theta_{1b}(\theta_1 - \theta_{1b})]}$$

$$\rightarrow (-\cot \theta_{1b}) \quad \text{as } \theta_1 \rightarrow \theta_{1b} ,$$

we obtain

$$\frac{\partial J}{\partial \eta} \Big|_{\eta \rightarrow 0} = v_1^2 \frac{1}{\left(\frac{\partial \eta}{\partial \theta_1}\right)^2} 2 \cos \theta_1 = J \frac{2 \cot \theta_1}{\left(\frac{\partial \eta}{\partial \theta_1}\right)} = -2J \frac{1}{\left(\frac{\partial \eta}{\partial \theta_1}\right)} \frac{\partial}{\partial \eta} \left(\frac{\partial \eta}{\partial \theta_1}\right) .$$

Then, in the expression for $\frac{dp}{d\eta} \Big|_{\eta=0}$, the coefficients in the terms involving

D_{\perp} cancel. Hence

$$\begin{aligned} \left. \frac{dp}{d\eta} \right|_{\eta=0} &= 2\pi \int_0^{\infty} dv_1 \text{JRD}_{\parallel} \left[-2 \frac{1}{\left(\frac{\partial \eta}{\partial \theta_1} \right)} \left[\frac{\partial}{\partial \eta} \left(\frac{\partial \eta}{\partial \theta_1} \right) \right] \left(\frac{\partial \eta}{\partial v_1} \right)^2 + 2 \left(\frac{\partial \eta}{\partial v_1} \right) \frac{\partial}{\partial \eta} \left(\frac{\partial \eta}{\partial v_1} \right) \right] \\ &= 2\pi \int_0^{\infty} dv_1 \text{JRD}_{\parallel} 2 \left(\frac{\partial \eta}{\partial v_1} \right) \left[- \frac{1}{\left(\frac{\partial \eta}{\partial \theta_1} \right)} \left[\frac{\partial}{\partial \eta} \left(\frac{\partial \eta}{\partial \theta_1} \right) \right] \left(\frac{\partial \eta}{\partial v_1} \right) + \frac{\partial}{\partial \eta} \left(\frac{\partial \eta}{\partial v_1} \right) \right] . \end{aligned}$$

Now the behavior of R and the value of $(\partial \eta / \partial v_1)$ makes the integral small.

Since R behaves exponentially, it drops very fast when v_1 is increasing. On the other hand, $\frac{\partial \eta}{\partial v_1} \propto \frac{\partial \theta_{1b}}{\partial v_1} \propto \cot \theta_{1b}$ which is very small when v_1 is small (because $\theta_{1b} \rightarrow \pi/2$ as $v_1 \rightarrow 0$). So we conclude that

$$\left. \frac{dp}{d\eta} \right|_{\eta=0} \approx 0 .$$

Acknowledgement

We gratefully acknowledge helpful discussions with J.D. Callen and R. Carrera. We also thank A.H. Futch and L.L. LoDestro for providing us with advance copies of their numerical results (Ref. 8). This work was supported by U.S. Department of Energy under contracts DE-AC02-78ET52048 and DE-AC02-80ER53104.

References

1. D.E. Baldwin and B.G. Logan, Phys. Rev. Lett. 43, 1318 (1979).
2. R.H. Cohen, J.B. Bernstein, J.J. Dornig, G. Rowlands, Nucl. Fusion 20, 1421 (1980).
3. G.A. Carlson et al., Lawrence Livermore National Laboratory Report UCRL-52836 (1979).
4. J. Kesner, Comments on Plasma Phys. and Cont. Fusion 5, 123 (1979); D.G. Braun and G.A. Emmert, University of Wisconsin Fusion Engineering Program Report UWFD-403 (1981).
5. G.W. Hamilton, Proc. 9th Symposium on Engineering Problems of Fusion Research (Chicago, IL, Oct. 26-29, 1981), Vol. 1, p. 700.
6. D.E. Baldwin, Sherwood Theory Meeting, April 1981.
7. X.Z. Li and G.A. Emmert, University of Wisconsin Fusion Engineering Program Report UWFD-393 (1980).
8. A.H. Futch and L.L. LoDestro, Lawrence Livermore National Laboratory, UCRL-87249 (1982).
9. R. Carrera and J.D. Callen, University of Wisconsin Fusion Engineering Program Report UWFD-466 (1982).
10. X.Z. Li and G.A. Emmert, University of Wisconsin Fusion Engineering Program Report UWFD-490 (1982).
11. V.P. Pastukhov, Nucl. Fusion 14, 3 (1974).
12. D.P. Chernin and M.N. Rosenbluth, Nucl. Fusion 18, 47 (1978).
13. P.J. Catto, I.B. Bernstein, Phys. Fluids 24, 1900 (1981).